Heliyon

ELSEVIER

*Received:*
21 April 2016
*Revised:*
1 July 2016
*Accepted:*
21 November 2016

Heliyon 2 (2016) e00203

# Aspartate-β-hydroxylase (ASPH): A potential therapeutic target in human malignant gliomas

**Lisa-Marie Sturla** [a,d,e,f,g,1], **Ming Tong** [a,h,1], **Nick Hebda** [e], **Jinsong Gao** [g,h], **John-Michael Thomas** [i], **Mark Olsen** [i], **Suzanne M. de la Monte** [a,b,c,d,e,f,g,h,*,1]

[a] *Liver Research Center, Providence, RI, United States*

[b] *Division of Gastroenterology, Providence, RI, United States*

[c] *Division of Neuropathology, Providence, RI, United States*

[d] *Department of Pathology, Providence, RI, United States*

[e] *Department of Neurology, Providence, RI, United States*

[f] *Department of Neurosurgery, Providence, RI, United States*

[g] *Department of Medicine, Providence, RI, United States*

[h] *Rhode Island Hospital and the Warren Alpert Medical School of Brown University, Providence, RI, United States*

[i] *Department of Pharmaceutical Sciences, College of Pharmacy-Glendale, Midwestern University, United States*

* Corresponding author at: Pierre Galletti Research Building, Rhode Island Hospital, 55 Claverick Street, Room 419, Providence, RI 02903, United States.

E-mail address: Suzanne_DeLaMonte_MD@Brown.edu (S.M. de la Monte).

[1] Authors contributed equally to this manuscript.

## Abstract

**Background:** Despite therapeutic advances, survival with glioblastoma multiforme (GBM) remains below 15 months from diagnosis due to GBM's highly infiltrative nature which precludes complete surgical resection. Patient outcomes could potentially be improved by targeting genes and pathways that drive neoplastic cell motility and invasiveness, including hypoxia-inducible factor-1 (HIF-1α), NOTCH, and aspartate-β-hydroxylase (ASPH).

**Methods:** Human astrocytoma biopsy specimens (n = 37), WHO Grades II–IV, were analyzed for levels and distributions of ASPH and HIF-1α immunoreactivity by immunohistochemical staining, and ASPH, Notch, JAG, HES1, HEY1 and HIF1α mRNA expression by quantigene multiplex analysis. The effects of small

http://dx.doi.org/10.1016/j.heliyon.2016.e00203

molecule inhibitors on ASPH's catalytic activity, cell viability and directional motility were examined in vitro in established GBM cell lines and primary tumor cells from an invasive mouse model of GBM.

**Results:** The highest grade astrocytoma, i.e. GBM was associated with the highest levels of ASPH and HIF1α, and both proteins were more abundantly distributed in hypoxic compared with normoxic regions of tumor. Furthermore, mining of the TCGA database revealed higher levels of ASPH expression in the mesenchymal subtype of GBM, which is associated with more aggressive and invasive behavior. In contrast, lower grade astrocytomas had low expression levels of ASPH and HIF1α. In vitro experiments demonstrated that small molecule inhibitors targeting ASPH's catalytic activity significantly reduced GBM viability and directional motility. Similar effects occurred in GBM cells that were transduced with a lentiviral sh-ASPH construct.

**Conclusion:** This study demonstrates that increased ASPH expression could serve as a prognostic biomarker of gliomas and may assist in assigning tumor grade when biopsy specimens are scant. In addition, the findings suggest that GBM treatment strategies could be made more effective by including small molecule inhibitors of ASPH.

Keywords: Medicine, Cell biology, Genetics, Neuroscience, Cancer Research

## 1. Introduction

In the United States, the annual incident rate of adult human primary brain tumors is about 17,000. Glioblastoma Multiforme (GBM) is the most common malignant primary brain tumor and despite advances in chemotherapy, neurosurgery, and radiation, median survival remains between 12 and 15 months following diagnosis [1, 2]. Furthermore, among all adult malignancies, GBM is the 4th highest in mortality, shortening life expectancy by an average of 23 years. Its aggressive migratory and infiltrating growth along the vessels, dendrites, and white matter fibers renders GBM difficult to resect and treat effectively. Novel measures are sorely needed to address these problems and improve therapeutic outcomes for GBM.

Several key pathophysiological processes are known to drive invasive growth of GBM. For example, necrosis and attendant hypoxia activate HIF-1α signaling, whilst amplification or constitutive activation of epidermal growth factor receptor (EGFR), platelet-derived growth factor receptor (PDGFR) and insulin-like growth factor receptor (IGFR) tyrosine kinases promote aggressive tumor cell growth and resistance to therapy. Enhanced NOTCH signaling, another prominent feature of GBM, drives cell proliferation, stem cell maintenance, tumor cell motility, and responses to hypoxia and angiogenesis [3]; the latter two correlate with aggressive and invasive tumor cell behavior. Beyond these molecules, aspartate-


http://dx.doi.org/10.1016/j.heliyon.2016.e00203

β-hydroxylase (ASPH; termed AAH in older literature) has been implicated in the cross-talk among all of these signaling pathways [4, 5, 6]. Correspondingly, ASPH is expressed at high levels in many malignant neoplasms of different histogeneses [4, 7, 8], and at very low levels or not at all in most normal cells and tissues, including brain [4, 5, 9, 10, 11, 12, 13]. ASPH's aggressive pro-tumor effects are mediated by gene over-expression, and/or high levels of its protein with attendant increased catalytic activity [4, 9, 14, 15]. Besides ASPH, Humbug, one of its isoforms that lacks a catalytic domain and has a probable role in cell adhesion/calcium flux, is also over-expressed in malignant neoplasms. Like ASPH, high levels of Humbug correlate with aggressive tumor cell behavior and worsened clinical prognosis [4, 8].

Given its importance as a potential biomarker and demonstrated prognosticator of clinical course, we designed the current study to determine the degree to which ASPH expression correlates with tumor grade, infiltrative growth, and progression-free survival in patients with astrocytomas. In addition, we sought to correlate ASPH expression with other molecular mediators of tumor cell motility and invasiveness, i.e. Notch and HIF-1α signaling networks. Furthermore, we mined data in The Cancer Genome Atlas (TCGA) database to assess associations between ASPH expression and molecular subtypes of GBM. Finally, we conducted in vitro experiments to determine the degree to which treatment of astrocytoma cells with small molecule inhibitors of ASPH's catalytic activity would be sufficient to decrease cell motility and invasion. The research design was focused on ASPH rather than Humbug because the Type 2 transmembrane structure of ASPH renders its critical catalytic domain accessible to small molecule inhibitor [15, 16] and immune [17, 18] targeting, as demonstrated in other malignancies.

## 2. Materials and methods

### 2.1. Ethics statement

The investigation was conducted in accordance with the ethical standards according to the Declaration of Helsinki, national and international guidelines and was approved by the institutional review board at Lifespan Academic Institutions.

### 2.2. Human subjects

Patients with biopsies or resections of newly diagnosed and untreated cerebral astrocytomas, WHO grade II, III, or IV were identified in the Rhode Island Hospital's surgical pathology archives between May 2011 and April 2012. Study inclusion criteria included availability of sufficient diagnostic tissue for molecular studies, and clinical follow-up data for at least 3 years since diagnosis. Patients


http://dx.doi.org/10.1016/j.heliyon.2016.e00203

were censored at time of tumor progression and death (with or without evidence of tumor progression).

Post-contrast, standard two-dimensional T1-weighted magnetic resonance imaging (MRI) studies were done pre- and post-surgery, and one month after completion of standard treatment with temozolomide and 60 Gy radiation. Thereafter, the MRI exams were repeated every two months until tumor progression or pseudo-progression was documented. Tumor progression was diagnosed based on modified Macdonald criteria [19] using post-contrast standard imaging as described above. Progressive disease was defined as clinical deterioration, the presence of new measurable, contrast-enhancing lesions, or a 25% increase in volume relative to previously measured enhancing lesions. Pseudo-progression was designated as transient contrast enhancement within the original radiation field that later stabilized or resolved. Volume enhancements of baseline post-operative and all subsequent post-operative MRI exams were computed using a constrained threshold-based segmentation strategy (IBSuite, Imaging Biometrics, Milwaukee, WI). Survival was calculated from the date of initial surgery.

## 2.3. Immunohistochemistry

Paraffin-embedded histological sections were immunostained to detect ASPH and HIF-1α as previously described [9, 11]. In brief, after deparaffinization in xylenes and rehydration through graded alcohol solutions, endogenous peroxidase was blocked by a 20-minute room temperature (RT) incubation in 0.6% $H_2O_2$ in methanol with gentle platform agitation. Non-specific binding sites were blocked by a 30-minute incubation in normal horse serum (1%). Adjacent sections were incubated with 1–2 μg/ml of mouse monoclonal antibodies to ASPH (A85G6 and A85E6) [20] or HIF1α (ab1-250 from Abcam, Cambridge, MA) over night at 4 °C. Immunoreactivity was detected using the avidin-biotin horseradish peroxidase complex system (Dako, Carpinteria, CA) following the manufacturer's protocol and using diaminobenzidine as the substrate. All incubations were carried out in humidified chambers. Between steps, slides were rinsed in three 5-minute changes of buffer (phosphate buffered saline) with gentle platform agitation. Slides were counterstained lightly with hematoxylin at the end of the immunostaining protocol. Tissue sections were preserved under coverglass using permanent mounting medium.

## 2.4. Quantigene 2.0 multiplex assay

RNA isolated from WHO grade III or IV astrocytomas was used in a custom designed Affymetrix multiplex assay to quantify mRNA transcripts encoding ASPH, HIF1α, and Notch associated signaling molecules. HPRT1 served as the


http://dx.doi.org/10.1016/j.heliyon.2016.e00203

internal control gene since its levels were invariant with glioma grade or the presence of a 17p/19q deletion. The assay was configured to utilize magnetic beads (Luminex) and a MAGPIX platform. After subtracting probe-related background from target median fluorescence intensity (MFI), results were normalized to HPRT1 and unpaired T-tests were used for intergroup statistical comparisons. In addition, Kaplan Meier curves generated with data from samples with low ASPH (MFI $<30$) versus high ASPH (MFI $>30$) expression were compared using the Mantel Cox log rank test.

## 2.5. TCGA gene expression analysis

To extend our analysis of ASPH expression in human gliomas in relation to GBM subtypes, we interrogated microarray platform results from a public database. This was accomplished by retrieving median expression data for 207 GBM samples used in the study by Verhaak et al. [21] via the TCGA data portal (https://tcga-data.nci.nih.gov/tcga). Sample data were rearranged to group tumors into the four TCGA defined molecular subclasses [21]. The TGCA database provides information about the molecular classification of tumors and overall survival, but not responsiveness to treatment. Sample data were rearranged to group tumors into the four TCGA defined molecular subclasses [22]. For further analysis, the resulting file was converted to a gct file that was compatible with the GenePattern software available from the Broad Institute (Cambridge, MA). We then compared the mean relative expression levels of all genes of interest across the four molecular subtypes of GBM (Table 1).

## 2.6. In vitro experiments

We used in vitro experiments to correlate ASPH expression with cell growth, viability, and motility, and examine the effects of small molecule inhibitors of ASPH's catalytic activity on glioma cell motility. Two experimental models were used: established human GBM cell lines including A172 and U87 (ATCC), and murine WTEGFR and EGFRVIII GBM cells derived from unique in vivo invasive models of GBM [23]. The WTEGFR cell line was induced by WTEGFR/TGFA expression, and the EGFRVIII cells were derived by inducing the mouse model with the EGFRVIII construct. Both cell lines were provided as a generous gift from Dr. A. Charest (Department of Neurosurgery, Tufts University Medical Center). All cell lines were maintained in Dulbecco's modified Eagle's medium supplemented with 4.5% glucose, 10% Fetal Bovine Serum, 4 mM glutamine and 100 mg/ml penicillin and streptomycin (Invitrogen, Carlsbad, CA, USA), and incubated at 37C in a standard humidified $CO_2$ incubator.


http://dx.doi.org/10.1016/j.heliyon.2016.e00203

**Table 1.** Genes and Gene Products Studied.

| Gene/Protein | Function |
|---|---|
| GFAP | Astrocyte specific cytoskeletal gene |
| HIF-1α | Transcription factor, key mediator of cellular response to hypoxia/stress |
| ASPH | Hydroxylates proteins containing EGF-like domains, including NOTCH, regulating activity |
| NOTCH1 | Key role in CNS development, cell motility and cell fate decisions |
| JAG1 | Ligand for NOTCH 1 |
| HES1 | Transcriptional target of NOTCH, regulates cell fate via transcriptional repression (key role in maintenance of neural stem cells) |
| HEY1 | Transcriptional target of NOTCH with a role in neurogenesis |
| HPRT1 | Hypoxanthine phosphoribosyltransferase 1, used widely as a housekeeping gene |

Abbreviations: GFAP = glial fibrillary acidic protein; HIF-1α= hypoxia-inducing factor-1 alpha; ASPH = aspartyl-β-hydroxylase; JAG1 = Jagged1; HES = Hairy and enhancer of split-1; HEY = Hairy/enhancer-of-split related with YRPW motif protein 1.

## 2.7. ASPH inhibitor experiments

Small molecule chemical inhibitors of ASPH were used to examine effects of ASPH inhibition of GBM cell viability and motility. Exploratory studies screened a panel of 14 MO-Is to assess their effects on GBM cell viability (Alamar blue assay). The small molecules included in the MO-I panel were independently shown to inhibit ASPH's catalytic activity (provided by Dr. Mark Olsen) [15]. The goal of the initial screening was to select suitable MO-Is and optimize the culture treatment doses for subsequent experiments aimed at characterizing their inhibitory effects on GBM viability, expression of ASPH, and directional motility, as previously described [7, 15]. We identified 4 (MO-I-1100, MO-I-400, MO-I-500 and MO-I-1151) that had efficacy in GBM cells.

### *2.7.1. Cell viability assay*

Cell viability was measured using the Alamar Blue assay (Promega, Madison, WI) according to the manufacturer's protocol. In brief, sub-confluent 96-well cultures were treated with vehicle (DMSO) or a single MO-I for 24 or 48 with daily changes of the medium and fresh addition of the MO-I. Alamar blue was added directly to the cultures, and after 3 hours incubation at 37 °C, fluorescence intensity was measured (Ex570/Em585 nm; arbitrary Relative Fluorescence Units = RFU). Six replicate cultures were assayed per treatment. Inter-group comparisons were made by one-way ANOVA with post hoc Tukey significance tests.


http://dx.doi.org/10.1016/j.heliyon.2016.e00203

### 2.7.2. Directional motility assay

Directional cell motility was measured using the 24-well Boyden chamber type Cytoselect cell migration and invasion assay (Cell Biolabs Inc., San Diego, CA) according to manufacturer's protocol. In brief, cells seeded in 10 cm plates were treated for 24 hours with vehicle or one of the inhibitors. The treated cells were then harvested and re-suspended in serum free media ($0.5 \times 10^6$ cells/ml). Full media containing 10% FBS was added as a trophic agent in the wells, below the culture inserts. 300 μl of the cell resuspensions were added to the culture inserts. After 6 hours incubation at 37 °C, the media from the culture inserts was removed by aspiration and non-migrated cells adherent to the inner surface of the culture insert membrane were removed with a cotton tip swab. The culture inserts were fixed, stained, and then dried. Cellular stain was eluted and absorbance (560 nm), which correlates linearly with cell number, was measured in a SpectraMax M5 microplate reader (Molecular Devices, Sunnyvale, CA). Six replicate assays per condition were used for statistical comparisons.

### 2.7.3. Western blot analysis

ASPH protein expression was measured by Western blot analysis as previously described [4]. Polyclonal ASPH antibody [16] was generated and characterized by 21st Century Biochemicals, Inc. (Marlboro, MA) using recombinant protein. The antibody binds to epitopes within both the N-terminus and C-terminus of the protein [16]. The N-terminus is virtually identical to Humbug, whereas the C-terminus is specific for ASPH [24]. The full length of ASPH is ~86 kD. However, Humbug and ASPH spontaneously cleave in vivo, resulting in several bands between ~35 kD and ~56 kD. Moreover, ASPH is phosphorylated by GSK-3β, resulting in upward shifts in Mr, including at ~140 kD [20]. Polyclonal anti-ASPH, which recognizes both N- and C-terminal domains, was used in these experiments because the monoclonal antibodies were generated in mice, and one goal was to compare effects of small molecule catalytic inhibitors on ASPH expression in murine and human GBM cell lines.

In brief, cultured cells were lysed in Pierce RIPA buffer (Thermo Scientific, Rockford, IL, USA) containing a protease inhibitor cocktail and 100 μg/ml PMSF, and lysates were clarified by centrifugation at 14,000xg for 15 min at 4 °C. The supernatants were used for Western blotting. Protein concentrations were measured using the bicinchoninic (BCA) assay (Pierce; Thermo Scientific). Samples containing 30 μg protein were fractionated by SDS-PAGE under reducing conditions. Proteins transferred to nitrocellulose membranes were blocked in Superblock-TBS (Thermo Scientific) and probed with rabbit polyclonal antibody to ASPH (1:1000) by overnight incubation at 4 °C with gentle platform agitation. Immunoreactivity was detected with horseradish peroxidase conjugated goat anti rabbit antibody (1:10,000; 1hr, room temperature) followed by Pierce Supersignal


http://dx.doi.org/10.1016/j.heliyon.2016.e00203

West Pico chemiluminescence reagent (Thermo Scientific). ASPH antibody was diluted in Tris-buffered saline containing 0.05% Tween-20 and 0.5% BSA (TBST-BSA), and goat anti-rabbit secondary antibody was diluted in TBST containing 0.5% casein. Membranes were washed at room temperature with 3 changes of TBST with gentle platform agitation.

## 2.8. sh-ASPH experiments

To confirm that the responses to the MO-Is were mediated by inhibition of ASPH, additional experiments examined effects of sh-ASPH on GBM cell viability and directional motility. To generate lentivirus-sh-ASPH (Lenti-sh-ASPH) and lentivirus-empty vector (Lenti-EV), 80% confluent HEK-293T cell cultures (10 cm-diameter dishes) were co-transfected with 15 μg of lentivirus sh-ASPH target construct (lentivirus PLK 0.1 sh-ASPH; Clone ID: TRCN0000053358, Dharmacon, Lafayette, CO) or control plasmid EV (lentivirus PLK 0.1 EV; Dharmacon, Lafayette, CO), 5 μg of pMD2.G (which contains VSVg), and 8.5 μg of psPAX2 (which contains GAG, POL) using the TransIT®-LT1 Reagent from Mirus Bio LLC. (Madison, WI). The pMD2 G and pSPAX2 (Addgene, Cambridge, MA) served as envelope and packaging plasmids. The cultures were incubated at 37 °C in a 5% $CO_2$ incubator. Medium containing Lenti-sh-ASPH or Lenti-EV was collected 48 hours after transfection and filtered (0.45 μm) prior to use. The ASPH target sequence was: ATTCACATTGTAGAGTGAGCG.

### *2.8.1. Lenti-sh-ASPH and Lenti-EV transductions*

U87 and A172 cells seeded into 6-well plates were incubated overnight to achieve 40% to 60% confluency. After vacuum suctioning the culture medium, the cells were incubated with 2 ml/well of Lentivirus stock (Lenti-sh-ASPH or Lenti-EV) diluted 1:2 in medium containing 10% FBS plus polybrene (final concentration 6 μg/ml). 24 hours post-transduction, the medium was replaced with fresh medium containing 10% FBS and 1 μg/ml puromycin. The cells were used in experiments 72 hours post-transduction. Exploratory studies determined that the 72-hour time point was optimum for ASPH inhibition and minimizing cell loss due to attendant impairments in cell adhesion.

### *2.8.2. Measurement of ASPH immunoreactivity in transduced cells*

ASPH protein expression in U87 and A172 cells transduced with Lenti-sh-ASPH or Lenti-EV was examined by Western blot analysis and duplex enzyme-linked immunosorbent assay (ELISA) [25]. The primary antibodies used to detect ASPH included polyclonal anti-ASPH, and the A85G6 and A85E6 monoclonal antibodies. Polyclonal anti-ASPH broadly detects ASPH, Humbug, and related cleavage products. A85E6 detects the N-terminal region of ASPH and Humbug.


http://dx.doi.org/10.1016/j.heliyon.2016.e00203

A85G6 detects the C-terminal region of ASPH present in the full-length protein and cleavage products. Since Humbug's amino acid sequences are identically represented in the N-terminal region of ASPH, it is not possible to distinguish Humbug from a cleavage product of ASPH that has the same size as Humbug. However, ASPH is distinguished from Humbug based on Mr (~86 kD and ~140 kD) and its immunoreactivity to A85G6.

Western blotting was performed as described earlier except that 40 μg instead of 30 μg of sample protein were loaded per lane, and the p85 subunit of PI3 kinase was used as a loading control. For the duplex ELISAs, 100 ng protein in 50 μl Tris buffered saline (TBS) were adsorbed to the bottoms of 96-well MaxiSorp plates by overnight incubation at 4 °C, and blocked for 3 hours with 1% bovine serum albumin (BSA) in TBS containing 0.05% Tween-20 (TBST). The samples were incubated with the A85G6 or A85E6 monoclonal antibody (0.1 μg/ml) for 1 hour at 37 °C. Immunoreactivity was detected with HRP-conjugated secondary antibody and the Amplex UltraRed soluble fluorophore. Fluorescence intensity was measured (Ex 565 nm/Em 595 nm) in a SpectraMax M5 microplate reader (Molecular Devices, Sunnyvale, CA). After rinsing in TBST, the samples were incubated with biotin-conjugated antibodies to large ribosomal protein (RPLPO), and immunoreactivity was detected with streptavidin-conjugated alkaline phosphatase (1:1000) followed by the 4-Methylumbelliferyl phosphate (4-MUP) fluorophore. Fluorescence (Ex360/Em450) was measured in a SpectraMax M5. Binding specificity was determined from parallel control incubations in which the primary or secondary antibody was omitted. The ratios of immunoreactivity corresponding to specific protein/RPLPO were calculated and used for inter-group comparisons [25, 26].

### *2.8.3. Viability and motility assays with Lenti-transduced cells*

Crystal violet dye or methylthiazolyidiphenyl-tetrazolium (MTT) reagents were used to measure effects of sh-ASPH on GBM viability in Lenti-transduced cells cultured for 24 hours in 96-well plates ($2 \times 10^4$ cells/well). Crystal violet is a vital dye that is only taken up by live cells. After labeling, the cells were thoroughly washed in PBS, then lysed in PBS containing 0.1% Tween-20. The MTT assay, which measures cell viability and mitochondrial function, was performed using commercial reagents according to the manufacturer's protocol (Sigma-Adrich, St. Louis, MO). Absorbances for CV (540 nm) and MTT (570 nm) were measured in a SpectraMax M5.

Directional motility was measured using the ATP luminescence-based motility and invasion (ALMI) assay [27]. The ALMI assay is similar to the Cytoselect assay described earlier with the following exceptions: 1) cells were seeded into each upper chamber in medium containing 0.1% FCS; 2) medium containing 1% FBS


http://dx.doi.org/10.1016/j.heliyon.2016.e00203

plus 10 ng/ml IGF-1 was supplied as the trophic factor in the lower chamber; 3) the upper and lower chambers were separated by 12 μm pore diameter polycarbonate filters; 4) cells were allowed to migrate for 30 minutes at 37 °C in a $CO_2$ incubator; 5) cells harvested from the upper surface/chamber (non-motile), under surface of the membrane (motile adherent), and lower chamber (motile non-adherent) were quantified using the ATPlite assay (PerkinElmer, Warwick, RI). Luminescence was measured in a TopCount (Packard Instrument Co., Meriden, CT). The calculated percentages of motile and non-motile cells were used in statistical analysis. ATP luminescence linearly correlates with cell number over a broad range [27], and with the short duration of the assay, the contributions of cell proliferation to changes in ATP content were likely to have been negligible.

## 2.9. Data analysis

Statistical analyses were performed using GraphPad Prism 6.0 software (San Diego, CA). Kaplan Meier survival curves generated with data from samples with low versus high ASPH expression were compared using the Mantel Cox log rank test. Inter-group comparisons of mean levels of gene expression, immunoreactivity, or motility were made using one-way or two-way ANOVA and the post hoc Tukey significance test. Alternatively, for two-way group comparisons, data were analyzed using unpaired T-tests.

# 3. Results

## 3.1. ASPH is more highly expressed in GBM than diffuse astrocytoma

Formalin-fixed paraffin embedded histological sections of 11 human GBM (Fig. 1A1–A4) and 11 diffuse astrocytoma (Fig. 1A5–A8) were stained with Hematoxylin and eosin (H&E) (Fig. 1A1 and A5), while adjacent sections were immunostained to detect the Ki-67 marker of cellular proliferation (Fig. 1A2 and A6), the astrocyte intermediate filament, glial fibrillary acidic protein (GFAP) (Fig. 1A3 and A7), and ASPH using the A85G6 + A85E6 monoclonal antibodies (Fig. 1A4 and A8). The study included 11 GBMs and 11 diffuse astrocytomas. ASPH protein was found to be more highly expressed in GBM than in diffuse astrocytoma. Higher levels of ASPH immunoreactivity were associated with higher cell densities, proliferation indices (Ki-67 nuclear labeling), and GFAP immunoreactivity.

Since ASPH expression has been linked to HIF-1α, the ASPH protein expression levels were compared in hypoxic (Fig. 1B6–B10) and normoxic (Fig. 1B1–B5) regions in the same GBMs. Locally hypoxic regions were characterized by the presence of pseudo-palisading necrosis (Fig. 1B6 versus B1), higher proliferation indices (Fig. 1B7 versus B2), and higher levels of HIF-1α expression (Fig. 1B10


http://dx.doi.org/10.1016/j.heliyon.2016.e00203

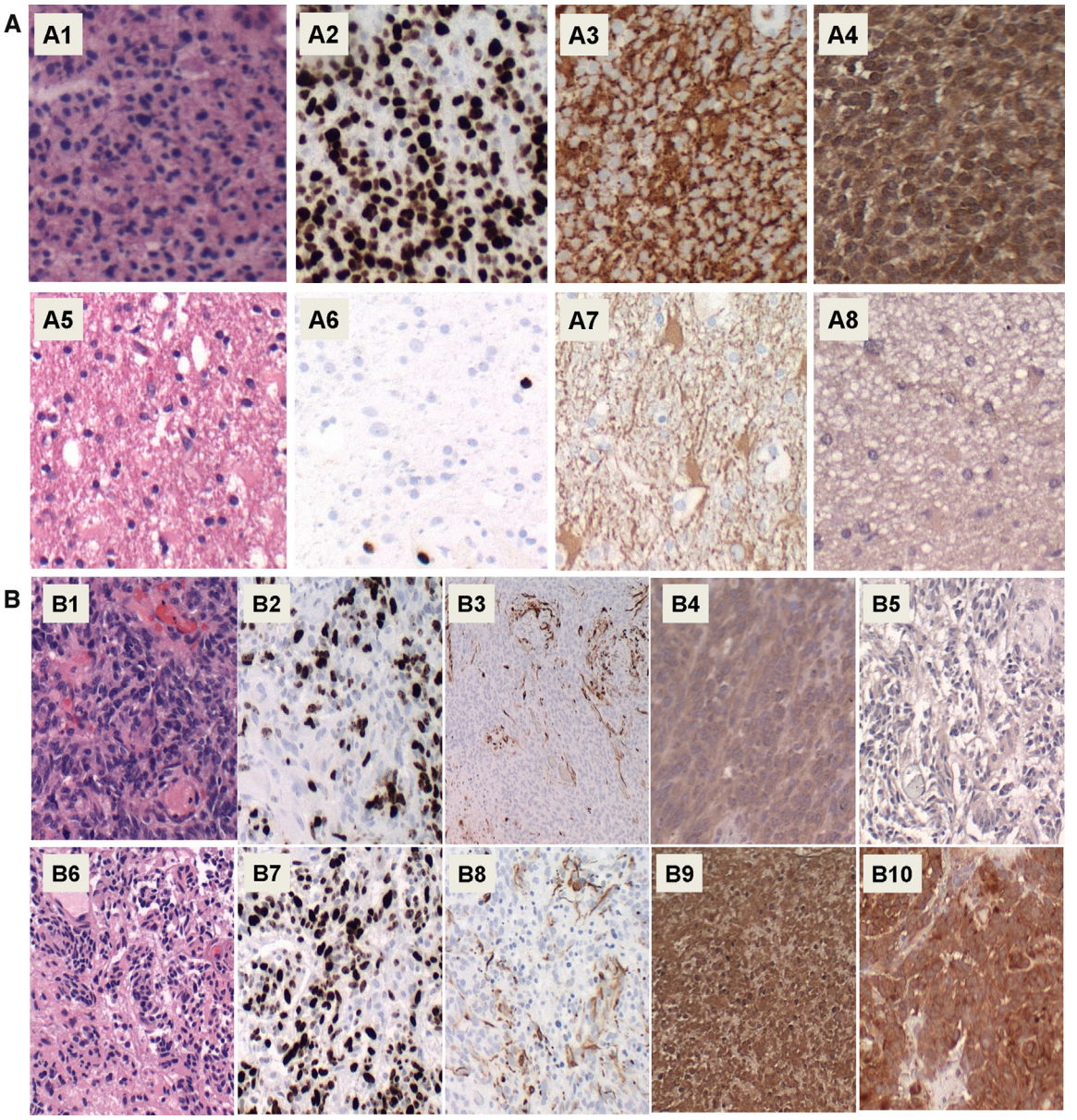


**Fig. 1.** ASPH expression in relation to [A] glioma grade and [B] effects of normoxic versus hypoxic environments: Formalin-fixed paraffin embedded histological sections of human [A1–A4] GBM and [A5–A8] diffuse astrocytoma were stained with [A1, A5] H&E, or immunostained to detect [A2, A6] Ki-67 proliferation marker, [A3, A7] GFAP astrocytic marker, and [A4, A8] ASPH. The study included 11 GBMs and 11 diffuse astrocytomas; representative results are shown. [B] Within the GBMs, representative [B1–B5] normoxic and [B6–B10] hypoxic regions of the same specimen are shown. Adjacent sections were stained with [B1, B6] H&E, or immunostained for [B2, B7] Ki-67, [B3, B8] GFAP, [B4, B9] ASPH, or [B5, B10] HIF-1α. Original magnification, 100x.

versus B6). ASPH expression was higher in hypoxic (Fig. 1B9) compared with normoxic (Fig. 1B4) regions of GBM. In contrast, the levels of GFAP immunoreactivity were similar in hypoxic (Fig. 1B8) compared with normoxic (Fig. 1B3) regions of GBM. The limited availability and archival nature of the


http://dx.doi.org/10.1016/j.heliyon.2016.e00203

paraffin-embedded human biopsy samples precluded further characterization of ASPH protein expression, such as by Western blot analysis.

## 3.2. Higher ASPH expression levels are associated with shortened survival with GBM

To correlate ASPH expression levels with survival, the tumors were categorized as low-level when median fluorescence index (MFI) measured by image analysis was less than 30 (n-20) or high-level when MFIs that were greater than 30 (n = 11). Kaplan Meier analysis demonstrated significantly shorter progression-free and overall survival durations in patients with high ASPH expressing GBMs (MFI >30) compared with those identified as having low ASPH expressing GBMs (MFI <30; log rank p = 0.005 and 0.0008 respectively; Fig. 2).

Patients were also divided into groups according to the presence or absence of pseudo-progression, which is a positive indicator of treatment response and correlated with longer overall survival [1, 22]. Patients who initially responded to

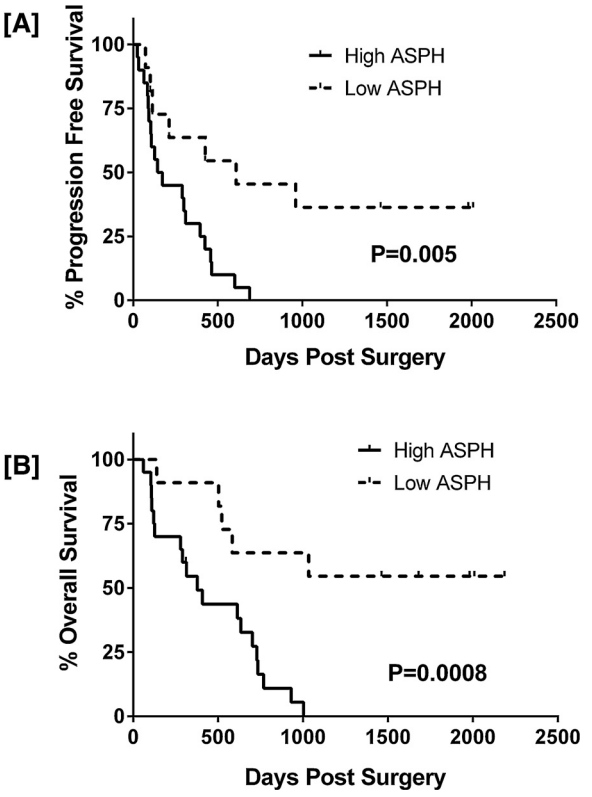


**Fig. 2.** Low ASPH expression is associated with longer progression-free and overall survival in GBM patients: Patients were grouped according to low (MFI <30; n = 20) or high (MFI >30; n = 11) levels of ASPH expression. Kaplan Meier analysis with post-hoc log rank analysis demonstrated significantly shorter [A] progression-free and [B] overall survival in patients with high ASPH expressing GBMs. Data reflect days post-surgery. Log rank p-values are shown in the panels.


http://dx.doi.org/10.1016/j.heliyon.2016.e00203

treatment then succumbed to disease had overall survivals of less than 6 months from diagnosis whereas those who developed pseudo-progression after their initial responses to treatment had a median overall survival of 23 months. Several patients within the pseudo-progression group remained alive with no evidence of disease progression for 4 years or more after surgery, or else they died 4 years or more post-surgery but with no evidence of disease progression.

### 3.3. Multiplex analysis demonstrated higher gene expression of ASPH and its signaling mediators in GBM patients with shorter progression-free and overall survival

To further characterize how survival correlates with expression of ASPH and related signaling molecules, mRNA levels of ASPH, HIF-1α, NOTCH1, JAGGED1, HES1, and HEY1 were measured in formalin-fixed paraffin-embedded GBM biopsy specimens using a custom multiplex assay (Fig. 3) (Table 2). Gene expression was normalized to the HPRT1 housekeeping gene. Subjects were grouped according to overall median survival durations of less than 6 months ($n = 21$), 23 months ($n = 10$), or greater than 48 months ($n = 6$). ASPH expression was 3.5-fold higher in patients who had overall survivals of less than 6 months ($n = 21$) when compared to those who had survived for at least 4 years ($n = 6$) ($p = 0.03$) (Fig. 3A). Similarly, HIF-1α, an upstream of ASPH, was more highly expressed in GBMs of patients with the shortest overall survival compared with those who survived for 4 years or more ($p = 0.03$) (Fig. 3B). Lower levels of ASPH and HIF-1α were also observed in the middle group ($n = 10$) in which the patients initially responded to treatment but later developed true tumor progression. Their median overall survival was 23 months, which was intermediate between the 6 months survival observed in patients with high ASPH/HIF-1α expressing GBMs and the

**Table 2.** ANOVA Tests of Inter-Group Differences in Gene Expression in Relation to Survival.

| Gene | F-Ratio | P-Value |
|---|---|---|
| ASPH | 4.073 | 0.0272 |
| NOTCH1 | 4.028 | 0.0269 |
| JAGGED1 | 4.000 | 0.0275 |
| HES1 | 5.382 | 0.0093 |
| HEY1 | 3.610 | 0.038 |
| HIF-1α | 4.404 | 0.0199 |

Gene expression was measured by a Quantigene 2.0-based RNA hybridization assay (see Methods). Results were analyzed by 1-way ANOVA and the Tukey multiple comparisons post-test. F-ratios and P-values reflect variances with respect to short (<6 months) versus intermediate (7–23 months) or long-term (>24 months) survival. Results with significant inter-group differences are shown in Fig. 4.


http://dx.doi.org/10.1016/j.heliyon.2016.e00203

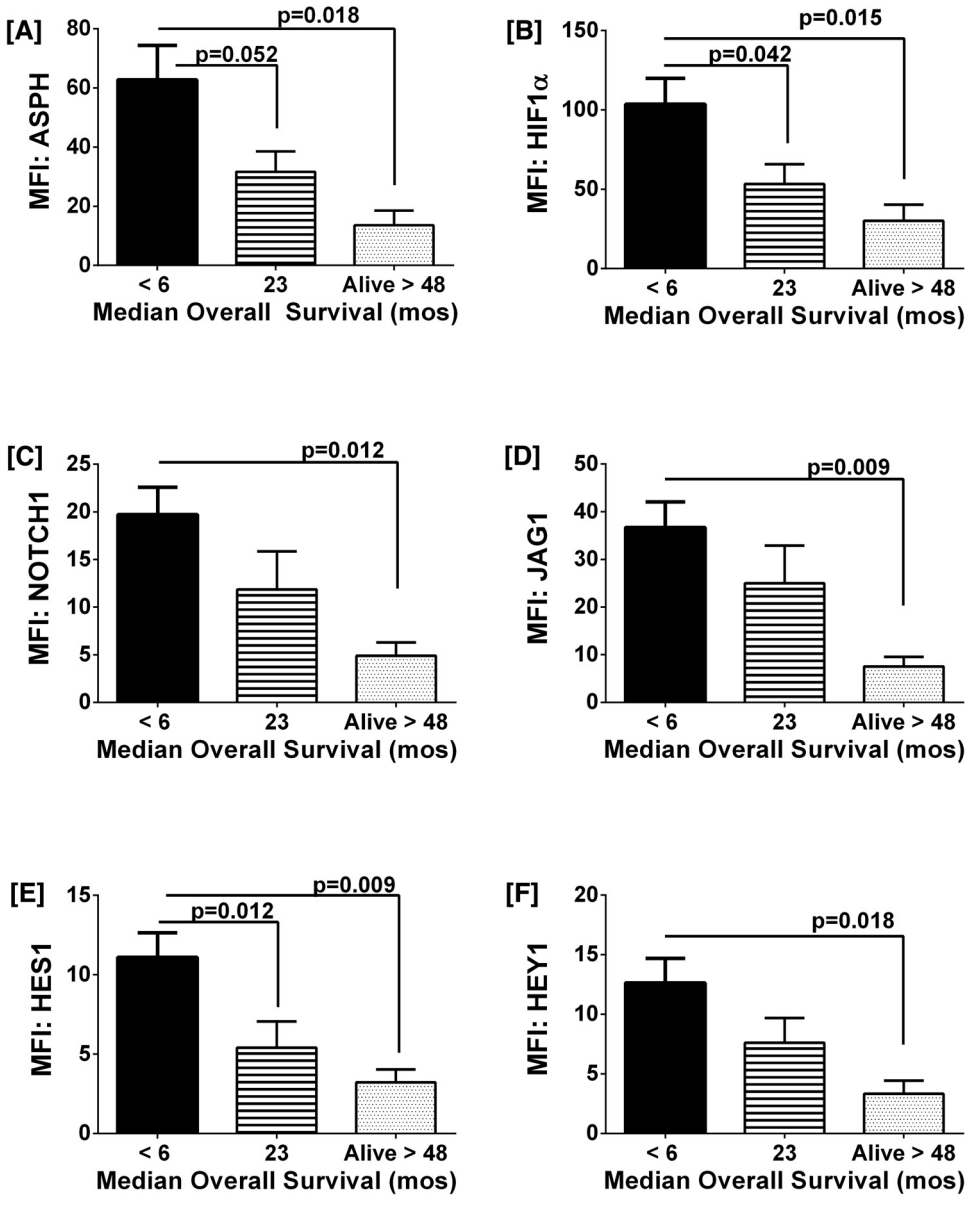


**Fig. 3.** Survival (treatment responsiveness) negatively correlates with gene expression levels of ASPH and related signaling mediators in GBM biopsy samples: RNA extracted from FFPE biopsy samples of GBM in patients with median survivals of <6 months (n = 21), 23 months (n = 10), or >48 months (n = 6) was used to measure mRNA levels corresponding to [A] ASPH, [B] HIF-1α, [C] NOTCH1, [D] JAGGED1, [E] HES1, and [F] HEY1 with a custom multiplex gene expression assay (Affymetrix). Results were normalized to housekeeping genes and mRNA levels are represented as median fluorescence index (MFI) ± SEM. Inter-group statistical comparisons were made by one-way ANOVA tests and post-hoc comparisons with the <6 month survival group.

greater than 4 years survival in patients with low ASPH/HIF-1α expressing GBMs. Corresponding with the results obtained for ASPH and HIF-1α, > 4 years survival was associated with significantly lower levels of NOTCH1 (Fig. 3C), JAGGED1 (Fig. 3D), HES1 (Fig. 3E) and HEY1 (Fig. 3F) expression in GBMs, whereas


http://dx.doi.org/10.1016/j.heliyon.2016.e00203

intermediate degrees of gene expression were measured in the subgroup with 23 months median survival.

## 3.4. ASPH and HIF-1α expression levels are elevated in mesenchymal subtypes of GBM

A recent study showed that enriched populations of circulating tumor cells in GBM patients expressed mesenchymal differentiation markers [28], and that a subpopulation of those cells was highly migratory. To extend our investigations to an independent and larger data source, we interrogated The Cancer Genome Atlas (TCGA; http://cancergenome.nih.gov) database and found that the ASPH gene is expressed in both neural and mesenchymal subtypes of GBM, and that the highest expression levels are associated with the aggressive mesenchymal subtype of GBM (Fig. 4A). Although ASPH is also elevated in the neural subgroup, a number of the other growth factors and cytokines that are responsible for mesenchymal transition are expressed at significantly lower levels (Fig. 4). Corresponding with the more aggressive behavior, mesenchymal GBMs with high levels of ASPH ($n = 59$) also expressed higher levels of HIF-1α ($n = 31$) compared with proneural ($n = 55$) or neural ($n = 53$) tumors ($p < 0.0001$ and $p < 0.001$, respectively) (Fig. 4B). Similarly, TGF-β1 expression was significantly increased in mesenchymal GBMs relative to proneural ($p < 0.0001$), neural and classical (both $p = 0.0001$) GBM subtypes (Fig. 4C).

## 3.5. Screening of small molecule inhibitors of ASPH's catalytic activity: One objective of these studies was to identify

Small molecule chemical inhibitors of ASPH (MO-Is) could potentially be used to inhibit growth and spread of GBMs in patients. To select the most effective MO-Is and optimize their doses for subsequent experiments, exploratory studies were used to screen a panel of 14 MO-Is (provided by Dr. Mark Olsen), assessing their inhibitory effects on A172 and U87 cell culture viability with the Alamar blue assay (Fig. 5). The small molecules included in the panel were independently shown to inhibit ASPH's catalytic activity [15]. Representative results graphed in Fig. 5 compare effects of 11 MO-Is: [A] MO-I-100, [B] MO-I-135, [C] MO-I-141, [D] MO-I-148, [E] MO-I-300, [F] MO-I-400, [G] MO-I-500, [H] MO-I-1000, [I] MO-I-1100, [J] MO-I-1200, and [K] MO-I-5000 on mean percentage change in viability. One consistent finding was that inhibitory effects on A172 cell viability were detected at the lowest doses (0.5 nM), whereas responses in U87 cells were more varied (including stimulatory). In addition, the inhibitory effects of the MO-Is were generally greater in A172 cells compared with U87 cells (Fig. 5). MO-I's that inhibited survival in both cell lines, i.e. MO-I-400, MO-I-500, MO-I-1100, MO-I-1151 (not shown) and MO-I-1200, were considered to have potential therapeutic value for GBM. These findings correspond with previous reports using the same


http://dx.doi.org/10.1016/j.heliyon.2016.e00203

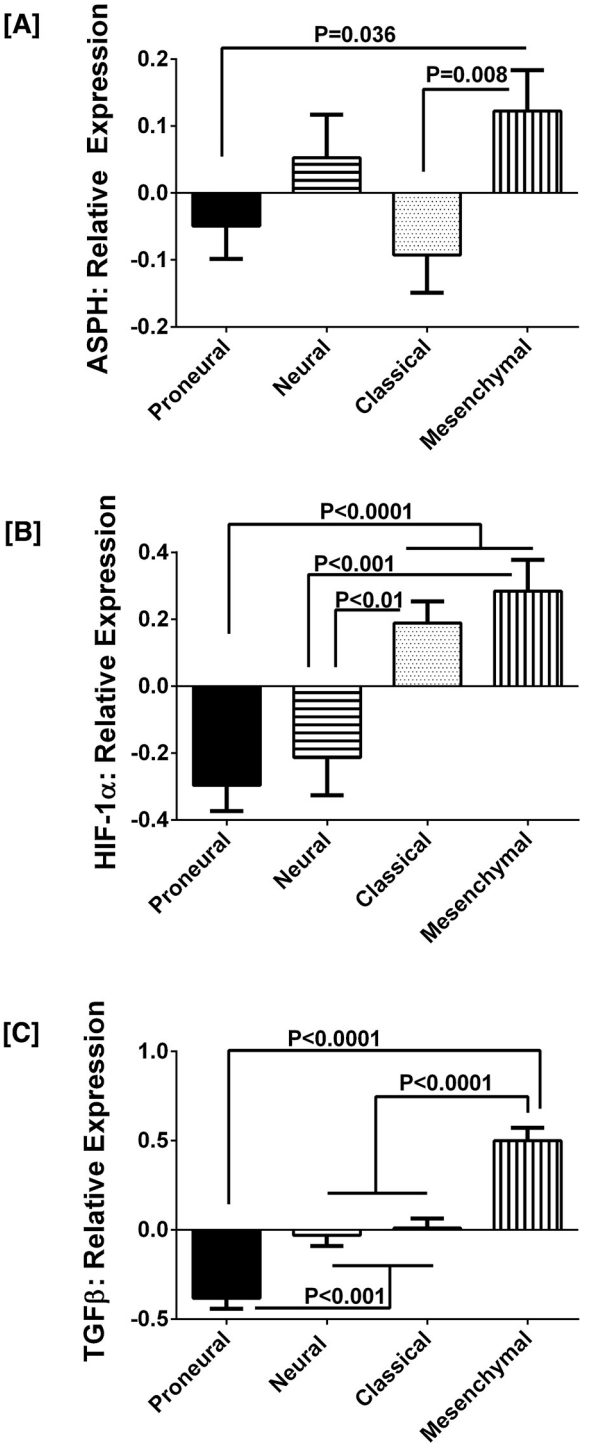


**Fig. 4.** ASPH, HIF-1α, and TGF-β1 expression levels are significantly higher in the more aggressive mesenchymal subtype of GBM: Analysis of TCGA data demonstrated significantly higher mRNA expression levels of [A] ASPH in mesenchymal compared with proneural and classical subtypes of GBM; higher levels of [B] HIF-1α in mesenchymal and classical compared with proneural and neural subtypes of GBM; and [C] higher levels of TGF-β1 in mesenchymal compared with proneural, neural, and classical GBM subtypes. Graphs depict relative mean ± S.E.M. levels of mRNA normalized to


http://dx.doi.org/10.1016/j.heliyon.2016.e00203

approach to interrogate effects of the MO-Is on viability and motility in other malignant neoplasms, [7, 15].

### 3.6. Small molecule inhibition of ASPH's catalytic activity significantly reduces cellular viability and directional motility in established GBM cell lines and primary experimental GBM cultures

Since ASPH has an important role in regulating tumor cell motility and invasiveness, and these ASPH functions are mediated via its catalytic domain, we hypothesized that selective ASPH inhibitors could be used to limit spread of GBMs. These in vitro experiments were conducted as proof of concept and designed to guide future in vivo experiments. Before conducting the small molecule inhibitor experiments, Western blot analysis was used to characterize basal expression ASPH and Humbug in human A172 and U87 cells (Fig. 6A), and in tumor cells derived from a highly invasive mouse GBM model (Fig. 6D).

A172 cells, which display mesenchymal morphology and aggressive cell growth [29, 30], had higher levels of ASPH expression (~86 kDa) than U87 cells; however Humbug, which mediates calcium flux from the ER, was more abundantly expressed in U87 compared with A172 cells (Fig. 6A). Tumor cells isolated from invasive genetic mouse models of GBM that have autocrine/paracrine activation of EGFR (WTEGFR/TGFA) expressed high levels of ASPH and Humbug, whereas cells that express a ligand-independent EGFR mutant (EGFRVIII) in the context of tumor suppressor loss, had lower levels of ASPH but similarly high levels of Humbug compared with WTEGFR/TGFA cells (Fig. 6D). Each Western blot lane was loaded with 30 μg of sample protein (measured using the BCA assay) and probed with polyclonal anti-ASPH. The blots were stripped and re-probed with anti-β-actin. Note that the mobility profiles of ASPH/Humbug and its fragments are not identical in human (Fig. 6A) and mouse (Fig. 6D) specimens, corresponding with their non-identical amino acid sequences.

Among the 5 MO-Is that had significant inhibitory effects on GBM cell viability (MO-I-400, MO-I-500, MO-I-1100, MO-I-1151, and MO-I-1200), the human GBM cells (A172 and U87) were most sensitive to MO-I-1100 whereas the murine GBM cells were most sensitive to MO-I-1151. Both MO-I-1100 and MO-I-1151 are under investigation in pre-clinical in vivo models of HCC [7]. Treatment of A172 cells with 5 μM or 20 μM MO-I-1100 for 48 hours reduced culture viability by 25% ($p < 0.0001$, $n = 6$) or 67% ($p < 0.0001$, $n = 6$) as demonstrated using the Alamar blue assay (Fig. 6B). Treatment of U87 cells with 5 μM or 20 μM MO-I-

housekeeping gene expression. Inter-group statistical comparisons were made by one-way ANOVA tests and the post-hoc Tukey multiple comparisons test.


http://dx.doi.org/10.1016/j.heliyon.2016.e00203

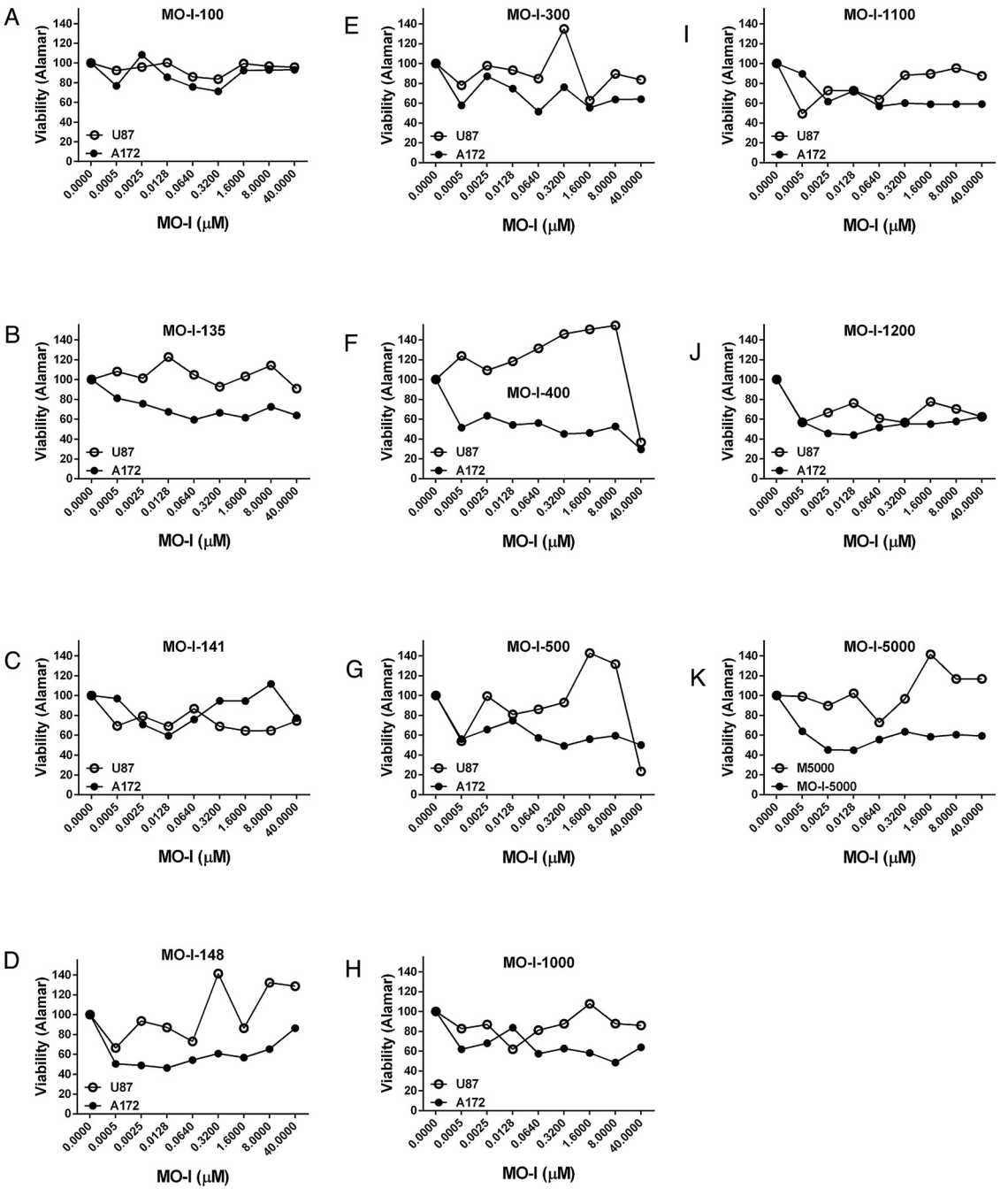


**Fig. 5.** Screening of Small Molecule Chemical Inhibitors of ASPH's catalytic activity in GBM cell lines: A panel of small molecule inhibitors of ASPH's catalytic activity (MO-I's) was screened in human GBM cell lines (A172 and U87) to select MO-I's for further analysis and optimize treatment doses based on their inhibitory effects on cell viability. Representative graphed data compare effects of: [A] MO-I-100, [B] MO-I-135, [C] MO-I-141, [D] MO-I-148, [E] MO-I-300, [F] MO-I-400, [G] MO-I-500, [H] MO-I-1000, [I] MO-I-1100, [J] MO-I-1200, and [K] MO-I-5000 on mean percentage change in viability of A172 (solid circles) and U87 (open circles) cells. Dose-effects of the MO-Is on cell viability were measured relative to corresponding vehicle-treated control cells using the Alamar blue assay.


http://dx.doi.org/10.1016/j.heliyon.2016.e00203

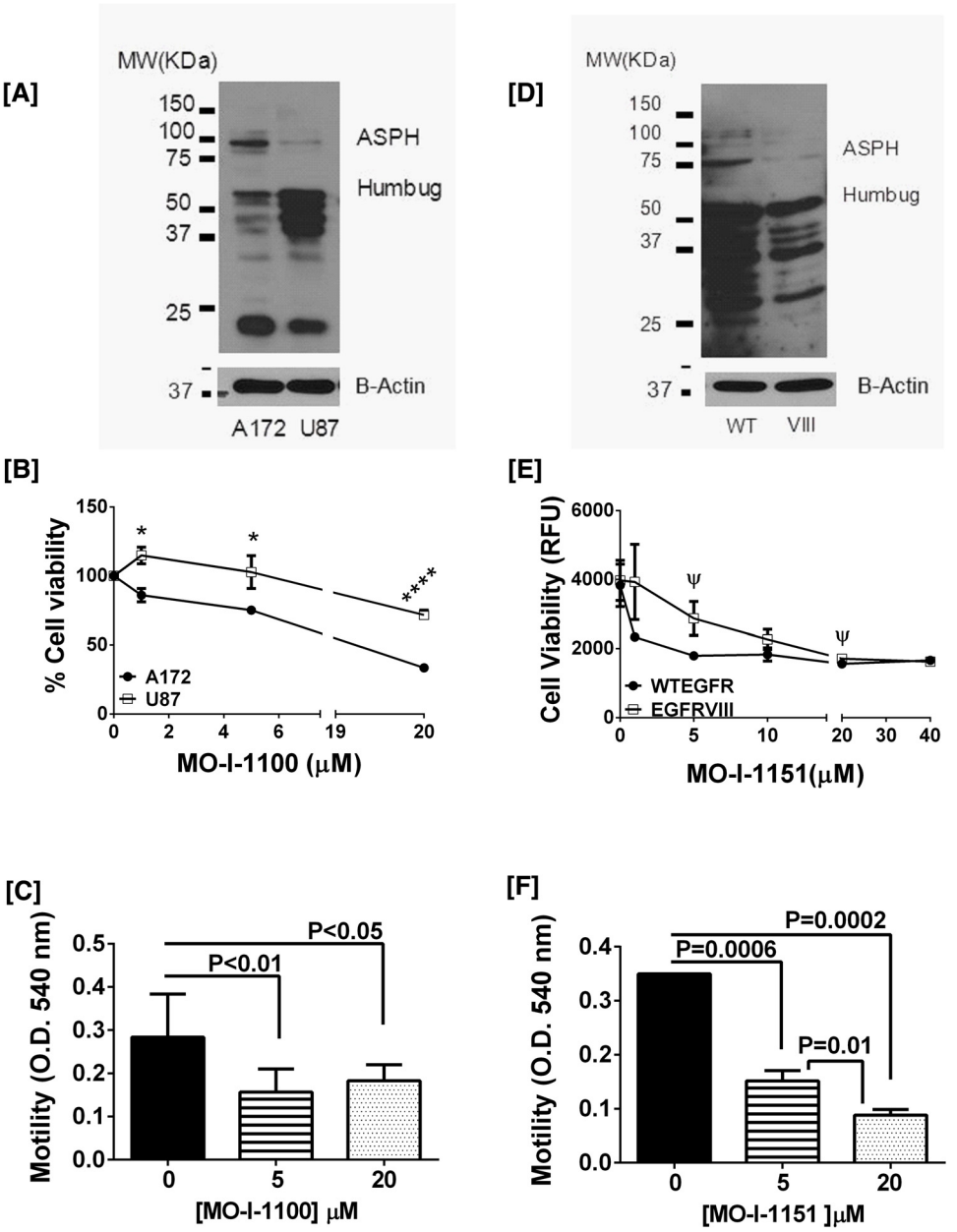


**Fig. 6.** Effects of Small Molecule Inhibition of ASPH on Viability of human and mouse GBM cell lines: ASPH immunoreactivity was demonstrated in [A] human A172 and U87 GBM, and [C] mouse WTEGFR (WT) and EGFRVIII (VIII) invasive GBM cell lines. Immunoreactivity was detected with rabbit polyclonal anti-ASPH which recognizes the ~86–140 kD ASPH (native and phosphorylated forms), as well as Humbug (~56 kDa) and its cleavage products shown in [A, D]. Blots were stripped and re-probed with antibodies to β-actin as a loading control. The differences in Western blot patterns between A and D are related to the non-identical amino acid sequences in human [A] and mouse [D]. [B, E] Sub-confluent cultures were treated for 48 hours with different concentrations (μM) of the MO-I-1100 or MO-I-1151 small molecule inhibitors of ASPH's catalytic activity. Cell viability was measured with the Alamar Blue colorimetric assay (mean ± S.E.M; n = 8/assay point). Inter-group comparisons were made by multiple T-tests with a false discovery rate of 1%. *$P < 0.01$; ****$P < 0.0001$; ψ $0.05 < P < 0.10$. Directional cell motility was measured in [C] A172 and [F] WTEGFR cells using a Boyden


http://dx.doi.org/10.1016/j.heliyon.2016.e00203

1100 for 48 hours reduced culture viability by 0% or 30% ($p < 0.0001$), respectively (Fig. 6B; $n = 6$). In essence, higher levels of sensitivity to MO-I-1100 correlated with higher levels of ASPH expression (Fig. 6A).

In the murine GBM experiments, both WTEGFR and EGFRVIII tumor cells were sensitive to MO-I-1151, although the dose-effects differed for the two cell lines. As noted for the human GBM cells, higher levels of ASPH expression correlated with greater sensitivity to MO-I-1151's inhibitory effects on cell viability. Treatment of WTEGFR cells with 5 μM MO-I-1151 for 48 hours decreased viability by 49% relative to vehicle ($p = 0.02$) (Fig. 6E). Higher concentrations of MO-I-1151 (20 μM or 40 μM) produced modest further reductions in cell viability, i.e. 53% relative to control ($p = 0.01$, $n = 4$). Corresponding with their lower levels of ASPH expression, EGFRVIII cells were less sensitive to MO-I-1151's inhibitory effects compared with WTEGFR cells such that twice the treatment dose, i.e. 10 μM instead of 5 μM was needed to significantly reduce culture viability by 41% ($p = 0.04$), and 40 μM was needed to reduce viability by 53 ($p = 0.008$%) (Fig. 6E). For each experiment using mouse GBM cells 4 independent cultures were analyzed per cell line and MO-I dose.

The effects of the MO-Is on directional cell motility were assessed using a trans-well chamber assay. Treatment with 5 μM MO-I-1100 significantly reduced directional motility of A172 cells by 43% relative to vehicle ($p = 0.02$, $n = 6$) (Fig. 6C). In addition, directional motility of WTEGFR-derived cells was significantly reduced by 57% ($p = 0.005$) and 74% (p-0.0008) following treatment with 5 μM and 20 μM MO-I-1151, respectively (Fig. 6F). These inhibitory effects of the MO-Is on directional motility were distinguishable from their reductions in viability because the motility assays included only viable cells and they were conducted over a 6-hour window, whereas the viability assays were conducted over a 48-hour period.

## 3.7. sh-ASPH inhibition of ASPH expression reduces viability and directional motility in GBM cells

Additional experiments using Lenti-sh-ASPH infected U87 and A172 cells were performed to confirm that inhibition of ASPH reduces GBM cell viability and motility. Polyclonal anti-ASPH, and monoclonal A85G6 and A85E6 antibodies were used for Western blot analysis to detect ASPH, and after stripping the blots, they were re-probed with polyclonal antibody to the p85 subunit of PI3 Kinase as a loading control (Fig. 7; also see Supplementary Figure 1 for full scale images of the blots). ASPH immunoreactivity was detected at ~140 kDa. Lower Mr bands

chamber type assay. Inter-group comparisons were made using one-way ANOVA with the post hoc Tukey multiple comparisons test.


http://dx.doi.org/10.1016/j.heliyon.2016.e00203

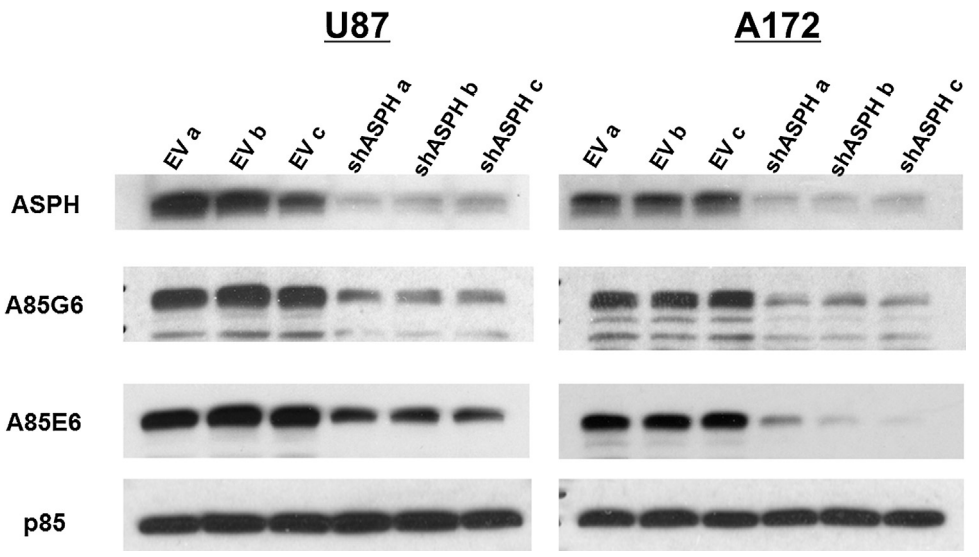


**Fig. 7.** Effects of sh-ASPH knockdown on ASPH expression: U87 and A172 human GBM cells were transduced with Lenti-sh-ASPH-RNA or empty vector (Lenti-EV) as a negative control and selected with puromycin. Western blot analysis was performed with polyclonal anti-ASPH, and the monoclonal A85G6 and A85E6 antibodies to examine effects of sh-ASPH on ASPH protein expression. Polyclonal anti-ASPH and A85E6 antibodies bind to the N-terminus of ASPH. However, those antibodies also detect Humbug since its amino acid sequences are virtually identical to those in the N-terminal region of ASPH. A85G6 binds to the C-terminus of ASPH which contains a catalytic domain that is not present in Humbug. All 3 antibodies can detect cleavage products of ASPH and Humbug. Each lane corresponds to an independent experiment using different preparations of the same Lenti-sh-ASPH or Lenti-EV construct. After probing ASPH, the blots were stripped and re-probed with antibodies to the p85 subunit of PI3 Kinase as a negative control (Also see Supplementary Figure 1).

corresponded to the expected sizes of Humbug or ASPH's cleavage products of (Supplementary Figure 1). For all 3 antibodies, Western blot analysis demonstrated that Lenti-sh-ASPH reduced ASPH protein expression in both U87 and A172 cells, whereas the levels of p85 immunoreactivity remained constant (Fig. 7A and B). In addition, the Western blot bands corresponding to Humbug had either similar intensities or only slightly reduced relative to Lenti-EV control infected cells (Supplementary Figure 1). Note that the higher overall Western blot signals in Fig. 7 relative to Fig. 6 were attributed to the use of 40 μg of protein per lane (Fig. 7) rather than 30 μg/lane (Fig. 6).

Duplex ELISAs using the A85G6 (Fig. 8A) or A85E6 (Fig. 8B) monoclonal antibody to ASPH demonstrated that cells transduced with Lenti-sh-ASPH had either significant or trend reductions in ASPH immunoreactivity compared with cells transduced with Lenti-EV, corresponding with the Western blot results. Crystal violet and MTT assays were used to measure effects of sh-ASPH on U87 and A172 cell viability. Crystal violet is a vital dye that only labels live cells. In contrast, the MTT assay measures both cell viability and mitochondrial function. U87 cells transduced with Lenti-sh-ASPH had significantly reduced Crystal Violet


http://dx.doi.org/10.1016/j.heliyon.2016.e00203

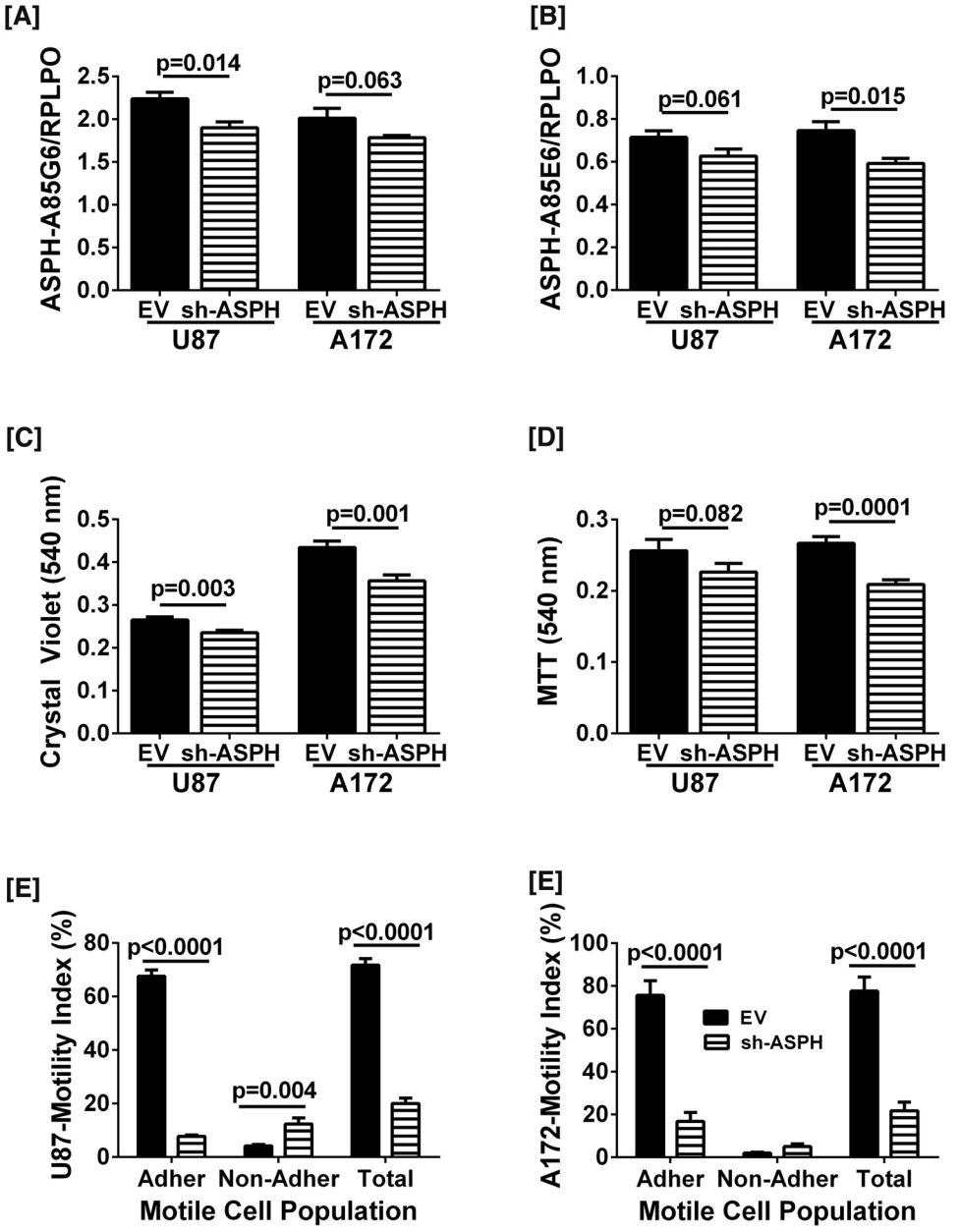


**Fig. 8.** Effects of sh-ASPH knockdown on GBM cell viability and directional motility: U87 and A172 human GBM cells were transduced with Lenti-sh-ASPH-RNA or empty vector (Lenti-EV) as a negative control and selected with puromycin. [A, B] Duplex ELISAs were performed with the A85G5 or A85E6 monoclonal antibodies to ASPH. Immunoreactivity was normalized to RPLPO. [C, D] Culture viability was measured in 8 replicate cultures with Crystal violet and MTT reagents. Graphs depict mean ± S.E. M. of results. Inter-group comparisons for each cell line were made using Student T-tests. Significant differences or trends are indicated over the bars. [E, F] Directional motility was measured in U87 and A172 cells using the ALMI assay (see Methods). Graphs depict motility indices corresponding to the calculated mean ± S.E.M. percentages of migrated adherent (located on the under surface of the filter), migrated non-adherent (distributed at the bottom of the blind well chamber), and total migrated (adherent + non-adherent) cells in 6 replicate assays per group. Inter-group comparisons were made by two-way ANOVA with post-hoc Tukey tests. Significant or trend p-values are shown.


http://dx.doi.org/10.1016/j.heliyon.2016.e00203

indices of viability (Fig. 8C) and trend reductions in MTT (Fig. 8D), whereas for the A172 cells, Lenti-sh-ASPH significantly reduced the mean levels of both CV and MTT (Fig. 8C and D). Therefore, inhibition of ASPH expression significantly reduced GBM viability.

The ATP-Lite Motility and Invasion (ALMI) assay was used to measure the effects of Lenti-sh-ASPH on directional motility, including in both adherent and non-adherent cell populations. The ALMI assay accounts for all cells in the Boyden-like chambers since ATP content, which is linearly correlated with cell number, is measured in non-migrated (remaining in the upper well of the chamber), migrated-adherent (migrated through the pores but adherent to the under-surface of the culture insert), and migrated-non-adherent (distributed at the bottom of the well) populations. The mean total motility indices (migrated-adherent + migrated non-adherent) of Lenti-sh-ASPH transduced U87 (Fig. 8E) and A172 (Fig. 8F) cells were significantly higher than corresponding cells transduced with Lenti-EV. Analysis of the motile cell subpopulations revealed that the main effect of sh-ASPH in both U87 and A172 cells was to significantly reduce the mean percentages of motile-adherent cells (Fig. 8E and F). In contrast, sh-ASPH either had no effect or it significantly increased the mean percentages of migrated non-adherent cells. The latter most likely reflects concurrent loss of cell adhesion functions in a subset of motile cells transduced with sh-ASPH. Given the short duration of the motility assay (30 minutes), the differential effects of Lenti-sh-ASPH could not be attributed to reductions in cell viability.

## 4. Discussion

Although progress has been made in characterizing molecular mechanisms of GBM development and behavior, further advances in therapeutics are needed to reduce GBM morbidity and mortality. The principle problem is that GBMs tend to be highly infiltrative, limiting surgical options and our ability to detect early stages of its spread. Therefore, an important consideration is the design therapeutic approaches that target mechanisms of GBM infiltration and invasiveness. ASPH cross-talks with several signaling pathways that drive invasive cell growth, motility, and invasion, including those that mediate infiltrative spread of GBM, e.g. hypoxia, HIF-1α, IGF1/2, and NOTCH [4, 8, 9] (Fig. 9). The ASPH, HIF-1α, NOTCH axis has been well characterized in hepatocellular carcinoma (HCC), neuroblastoma [12], PNET [5], and immature migratory cerebellar neurons [6]. The present study is the first to examine its expression in astrocytoma. Herein, we confirmed high levels or ASPH expression in high grade glioma (grade IV) at both the mRNA and protein levels. Immunohistochemical staining confirmed that higher levels of ASPH expression occurred in more aggressive GBMs compared with lower grade diffuse astroctyomas. Correspondingly, higher levels of ASPH correlated with increased cellularity (cell density) and proliferation indices as determined by Ki-67


http://dx.doi.org/10.1016/j.heliyon.2016.e00203

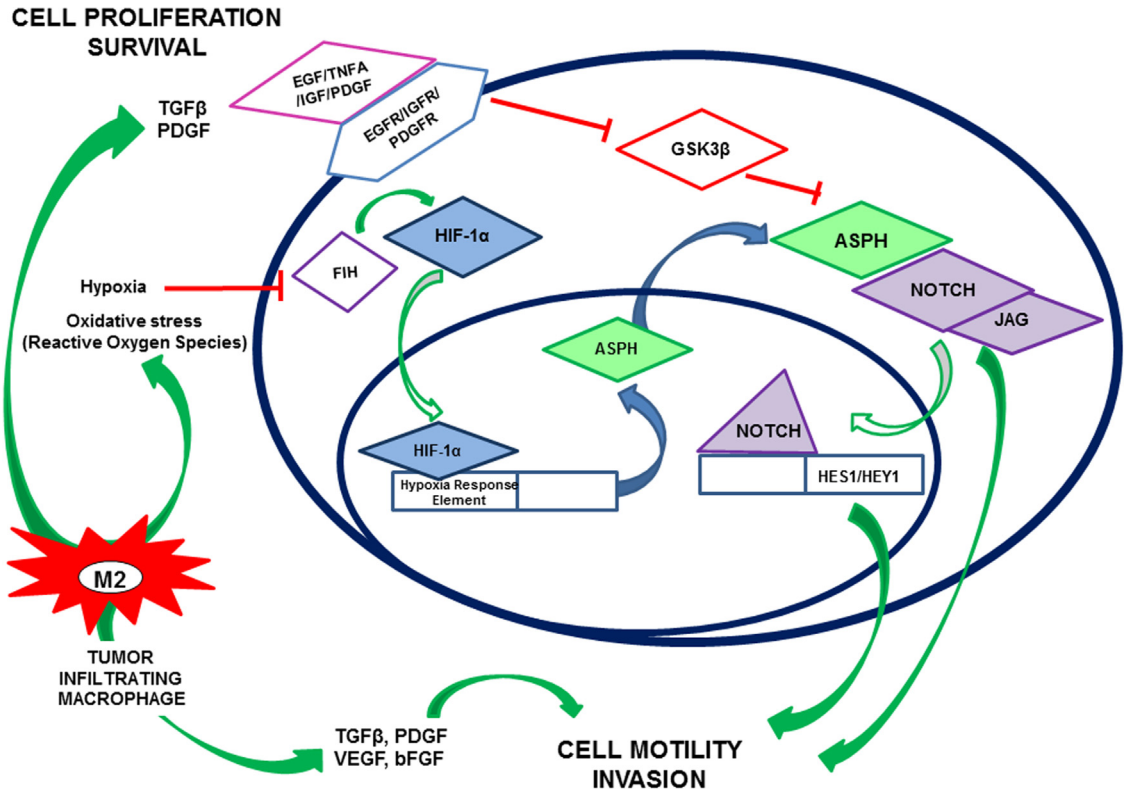


**Fig. 9.** Schematic representation of proposed role of ASPH in key signaling pathways responsible for infiltrative spread of GBM: Constitutive activation of epidermal growth factor receptor (EGFR), platelet-derived growth factor receptor (PDGFR) and insulin-like growth factor receptor (IGFR) tyrosine kinases promotes cellular attenuates GSK3β activity leading to enhanced ASPH expression and activity, and attendant increased activation of NOTCH signaling. Necrosis and associated hypoxia drive tumor-infiltrating macrophages to increase oxidative stress, activating HIF-1α signaling, which also increases ASPH expression. The consequent downstream enhancement of Notch signaling drives tumor cell motility and invasion.

nuclear staining indices. Finally, HIF-1α and ASPH were both more abundantly expressed in hypoxic compared with normoxic regions of the same GBM.

Invasive growth of tumor cells is regulated by the microenvironment and dependent upon interactions between the neoplastic cells and normal tissue elements and mechanisms that control remodeling. Epithelial-mesenchymal transition (EMT) is an adaptive process that mediates programmed changes in gene expression and function with phenotypic consequences [28]. This phenomenon has been well documented in epithelial tumors such as prostate and breast, and has been shown to have a regulatory role in causing cells to switch between proliferative and metastatic/invasive behavior [31] as occurs with progressive growth and spread of malignant neoplasms.

Hypoxia is a key mediator of this switch as it drives tumor cells away from proliferative behavior and towards invasive growth, angiogenesis, and eventually


http://dx.doi.org/10.1016/j.heliyon.2016.e00203

metastatic spread. Hypoxia is a prominent micro-environmental feature of astrocytomas. In high grade gliomas, particularly GBMs, rapid tumor cell growth, together with vascular thrombosis and hemorrhage, bolster oxygen requirements in the adjacent tumor-free tissue. Our analysis of the TCGA gene expression data showed both ASPH and HIF-1α are expressed at significantly higher levels in the mesenchymal subtype of GBM. This suggests that both ASPH and HIF-1α may be involved in the mesenchymal transition; this role for HIF-1α has already been described. Correspondingly, we observed that both ASPH and HIF-1α were most abundantly expressed in the most aggressive WHO grade IV gliomas, and that the expression levels of both were higher in hypoxic compared with normoxic regions of tumor. Together, these findings support our hypothesis that high levels of ASPH and HIF-1α expression correlate with more aggressive phenotypes of human gliomas.

Since hypoxic niches are well-known as sources of tumor initiation, i.e. glioma stem cells [32], it would be of interest to study ASPH activity in this cell population. Targeting ASPH expression or catalytic activity in glioma stem cells could provide an additional means of eradicating the source of otherwise treatment-resistant tumors responsible for GBM recurrence and progression. In previous publications, the MO-I small molecule inhibitors were demonstrated to target ASPH's catalytic (hydroxylase) activity and inhibiting cell motility [7, 15, 16]. In addition, a number of publications have documented that mutation of ASPH's catalytic domain [9, 33] inhibits cell motility in a broad range of malignant neoplastic cells. Furthermore, as demonstrated in the present work, GBM cells transduced with Lenti-sh-ASPH resulting in sustained inhibition of ASPH expression, exhibited reduced viability and directional motility. Correspondingly, si-RNA [5, 6, 34] or antisense oligonucleotides [12, 35] targeting ASPH and not Humbug, inhibit cell motility. Although catalytic activity was not specifically demonstrated to be inhibited by the MO-Is in the GBM cells, the most important consequence of inhibiting hydroxylase activity, i.e. cell motility [4, 12, 14], was significantly decreased by exposure to selected MO-Is.

Unlike many of the inter-related signaling molecules that also correlate with poor clinical outcome, ASPH is the most exciting potential therapeutic target because it is not expressed at appreciable levels in the normal mature brain or in most normal adult tissues [10, 36]. Therefore, therapeutic targeting ASPH in GBM and glioma stem cells is attractive given the likelihood of sparing normal brain. In this regard, as ASPH is a Type 2 trans-membrane protein that is expressed on the surface of malignant neoplastic cells [10], it is accessible to both immunotherapy and small molecule inhibition of its catalytic (hydroxylase) activity which is localized in the C-terminal domain. Correspondingly, we demonstrated reduced viability and directional motility in GBM cells treated with MO-Is targeting ASPH's catalytic


http://dx.doi.org/10.1016/j.heliyon.2016.e00203

site. Reduced viability via treatment with MO-Is was recently linked to enhanced tumor cell senescence [37]. What makes ASPH targeting in gliomas even more promising is that there is no evidence of mutation, and instead the gene and protein are over-expressed via cross-talk with other signaling pathways, e.g. insulin/IGF/IRS. Inhibiting ASPH expression and/or catalytic activity blocks NOTCH activation [5, 16] and cross-talk with HIF-1α [5], which promote cell motility and invasion. Conceivably, ASPH could represent a unique example of single-target therapy for GBM, particularly for preventing recurrence and controlling progression in the context of multi-drug resistance. Small molecule inhibitors of ASPH's hydroxylase activity have already proven to be effective in preclinical studies of HCC [7].

## Declarations

### Author contribution statement

Lisa-Marie Sturla, Suzanne de la Monte: Conceived and designed the experiments; Performed the experiments; Analyzed and interpreted the data; Wrote the paper.

Ming Tong, Nick Hebda: Performed the experiments.

Jinsong Gao: Conceived and designed the experiments; Performed the experiments.

Mark Olsen, John-Michael Thomas: Contributed reagents, materials, analysis tools or data.

### Competing interest statement

The authors declare no conflict of interest

### Funding statement

This work was supported by the National Institutes of Health (AA-11431 and AA-12908) and grants from the Rhode Island Hospital Neurology foundation and the Lura Cook Hull Trust.

### Additional Information

Supplementary content related to this article has been published online at http://dx.doi.org/10.1016/j.heliyon.2016.e00203

### Acknowledgements

The authors acknowledge Dr Alain Charest (Tufts University Medical Center, Boston, MA) for his generous donation of the mouse model derived cell lines for

this research. The authors also thank Moh Lik Roy Ang and Rafael Tua-Caraccia, undergraduate students at Brown University, for their participation in technical aspects of this research, and Dr. C.K. Huang for supplying critical reagents for generating the Lenti-sh-ASPH.

## References

[1] Roger Stupp, Warren P. Mason, Martin J. van den Bent, Michael Weller, Barbara Fisher, Martin J.B. Taphoorn, Karl Belanger, Alba A. Brandes, Christine Marosi, Ulrich Bogdahn, Jürgen Curschmann, Robert C. Janzer, Samuel K. Ludwin, Thierry Gorlia, Anouk Allgeier, Denis Lacombe, J. Gregory Cairncross, Elizabeth Eisenhauer, René O. Mirimanoff, for the European Organisation for Research and Treatment of Cancer Brain Tumor and Radiotherapy Groups and the National Cancer Institute of Canada Clinical Trials Group, Radiotherapy plus concomitant and adjuvant temozolomide for glioblastoma, N. Engl. J. Med. 352 (2005) 987–996.

[2] S.J. Hentschel, F.F. Lang, Current surgical management of glioblastoma, Cancer J. 9 (2003) 113–125.

[3] K.H. Plate, W. Risau, Angiogenesis in malignant gliomas, Glia 15 (1995) 339–347.

[4] M.C. Cantarini, S.M. de la Monte, M. Pang, M. Tong, A. D'Errico, F. Trevisani, J.R. Wands, Aspartyl-asparagyl beta hydroxylase over-expression in human hepatoma is linked to activation of insulin-like growth factor and notch signaling mechanisms, Hepatology 44 (2006) 446–457.

[5] M. Lawton, M. Tong, F. Gundogan, J.R. Wands, S.M. de la Monte, Aspartyl-(asparaginyl) beta-hydroxylase, hypoxia-inducible factor-alpha and Notch cross-talk in regulating neuronal motility, Oxid. Med. Cell. Longev. 3 (2010) 347–356.

[6] E. Silbermann, P. Moskal, N. Bowling, M. Tong, S.M. de la Monte, Role of aspartyl-(asparaginyl)-beta-hydroxylase mediated notch signaling in cerebellar development and function, Behav. Brain Funct. 6 (2010) 68.

[7] A. Aihara, C.K. Huang, M.J. Olsen, Q. Lin, W. Chung, Q. Tang, X. Dong, J. R. Wands, A cell-surface beta-hydroxylase is a biomarker and therapeutic target for hepatocellular carcinoma, Hepatology 60 (2014) 1302–1313.

[8] M. Luu, E. Sabo, S.M. de la Monte, W. Greaves, J. Wang, R. Tavares, L. Simao, J.R. Wands, M.B. Resnick, L. Wang, Prognostic value of aspartyl (asparaginyl)-beta-hydroxylase/humbug expression in non-small cell lung carcinoma, Hum. Pathol. 40 (2009) 639–644.

 http://dx.doi.org/10.1016/j.heliyon.2016.e00203

[9] N. Ince, S.M. de la Monte, J.R. Wands, Overexpression of human aspartyl (asparaginyl) beta-hydroxylase is associated with malignant transformation, Cancer Res. 60 (2000) 1261–1266.

[10] L. Lavaissiere, S. Jia, M. Nishiyama, S. de la Monte, A.M. Stern, J.R. Wands, P.A. Friedman, Overexpression of human aspartyl(asparaginyl)beta-hydroxylase in hepatocellular carcinoma and cholangiocarcinoma, J. Clin. Invest. 98 (1996) 1313–1323.

[11] T. Maeda, K. Taguchi, S. Aishima, M. Shimada, D. Hintz, N. Larusso, G. Gores, M. Tsuneyoshi, K. Sugimachi, J.R. Wands, S.M. de la Monte, Clinicopathological correlates of aspartyl (asparaginyl) beta-hydroxylase over-expression in cholangiocarcinoma, Cancer Detect. Prev. 28 (2004) 313–318.

[12] P.S. Sepe, S.A. Lahousse, B. Gemelli, H. Chang, T. Maeda, J.R. Wands, S.M. de la Monte, Role of the aspartyl-asparaginyl-beta-hydroxylase gene in neuroblastoma cell motility, Lab. Invest. 82 (2002) 881–891.

[13] S.A. Lahousse, J.J. Carter, X.J. Xu, J.R. Wands, S.M. de la Monte, Differential growth factor regulation of aspartyl-(asparaginyl)-beta-hydroxylase family genes in SH-Sy5y human neuroblastoma cells, BMC Cell Biol. 7 (2006) 41.

[14] S.M. de la Monte, S. Tamaki, M.C. Cantarini, N. Ince, M. Wiedmann, J.J. Carter, S.A. Lahousse, S. Califano, T. Maeda, T. Ueno, A. D'Errico, F. Trevisani, J.R. Wands, Aspartyl-(asparaginyl)-beta-hydroxylase regulates hepatocellular carcinoma invasiveness, J. Hepatol. 44 (2006) 971–983.

[15] X. Dong, Q. Lin, A. Aihara, Y. Li, C.K. Huang, W. Chung, Q. Tang, X. Chen, R. Carlson, C. Nadolny, G. Gabriel, M. Olsen, J.R. Wands, Aspartate beta-Hydroxylase expression promotes a malignant pancreatic cellular phenotype, Oncotarget 6 (2015) 1231–1248.

[16] C.K. Huang, Y. Iwagami, A. Aihara, W. Chung, S. de la Monte, J.M. Thomas, M. Olsen, R. Carlson, T. Yu, X. Dong, J. Wands, Anti-Tumor effects of second generation beta-hydroxylase inhibitors on cholangiocarcinoma development and progression, PLoS One 11 (2016) e0150336.

[17] Y. Tomimaru, S. Mishra, H. Safran, K.P. Charpentier, W. Martin, A.S. De Groot, S.H. Gregory, J.R. Wands, Aspartate-beta-hydroxylase induces epitope-specific T cell responses in hepatocellular carcinoma, Vaccine 33 (2015) 1256–1266.

[18] M. Shimoda, Y. Tomimaru, K.P. Charpentier, H. Safran, R.I. Carlson, J. Wands, Tumor progression-related transmembrane protein

 http://dx.doi.org/10.1016/j.heliyon.2016.e00203

aspartate-beta-hydroxylase is a target for immunotherapy of hepatocellular carcinoma, J. Hepatol. 56 (2012) 1129–1135.

[19] D.R. Macdonald, T.L. Cascino, S.C. Schold Jr., J.G. Cairncross, Response criteria for phase II studies of supratentorial malignant glioma, J. Clin. Oncol. 8 (1990) 1277–1280.

[20] S.M. de la Monte, M. Tong, R.I. Carlson, J.J. Carter, L. Longato, E. Silbermann, J.R. Wands, Ethanol inhibition of aspartyl-asparaginyl-beta-hydroxylase in fetal alcohol spectrum disorder: potential link to the impairments in central nervous system neuronal migration, Alcohol 43 (2009) 225–240.

[21] R.G. Verhaak, K.A. Hoadley, E. Purdom, V. Wang, Y. Qi, M.D. Wilkerson, C.R. Miller, L. Ding, T. Golub, J.P. Mesirov, G. Alexe, M. Lawrence, M. O'Kelly, P. Tamayo, B.A. Weir, S. Gabriel, W. Winckler, S. Gupta, L. Jakkula, H.S. Feiler, J.G. Hodgson, C.D. James, J.N. Sarkaria, C. Brennan, A. Kahn, P.T. Spellman, R.K. Wilson, T.P. Speed, J.W. Gray, M. Meyerson, G. Getz, C.M. Perou, D.N. Hayes, N. Cancer Genome Atlas Research, Integrated genomic analysis identifies clinically relevant subtypes of glioblastoma characterized by abnormalities in PDGFRA, IDH1, EGFR, and NF1, Cancer Cell 17 (2010) 98–110.

[22] S. Jeyapalan, J. Boxerman, J. Donahue, M. Goldman, T. Kinsella, T. Dipetrillo, D. Evans, H. Elinzano, M. Constantinou, E. Stopa, Y. Puthawala, D. Cielo, A. Santaniello, A. Oyelese, K. Mantripragada, K. Rosati, D. Isdale, H. Safran, Brown University Oncology Group Study, Paclitaxel poliglumex, temozolomide, and radiation for newly diagnosed high-grade glioma: a Brown University Oncology Group Study, Am. J. Clin. Oncol. 37 (2014) 444–449.

[23] H. Zhu, J. Acquaviva, P. Ramachandran, A. Boskovitz, S. Woolfenden, R. Pfannl, R.T. Bronson, J.W. Chen, R. Weissleder, D.E. Housman, A. Charest, Oncogenic EGFR signaling cooperates with loss of tumor suppressor gene functions in gliomagenesis, Proc. Natl. Acad. Sci. U. S. A. 106 (2009) 2712–2716.

[24] J.E. Dinchuk, N.L. Henderson, T.C. Burn, R. Huber, S.P. Ho, J. Link, K.T. O'Neil, R.J. Focht, M.S. Scully, J.M. Hollis, G.F. Hollis, P.A. Friedman, Aspartyl beta -hydroxylase (Asph) and an evolutionarily conserved isoform of Asph missing the catalytic domain share exons with junctin, J. Biol. Chem. 275 (2000) 39543–39554.

[25] L. Longato, K. Ripp, M. Setshedi, M. Dostalek, F. Akhlaghi, M. Branda, J.R. Wands, S.M. de la Monte, Insulin resistance, ceramide accumulation, and

 http://dx.doi.org/10.1016/j.heliyon.2016.e00203

endoplasmic reticulum stress in human chronic alcohol-related liver disease, Oxid. Med. Cell. Longev. 2012 (2012) 479348.

[26] L. Longato, M. Tong, J.R. Wands, S.M. de la Monte, High fat diet induced hepatic steatosis and insulin resistance: role of dysregulated ceramide metabolism, Hepatol. Res. 42 (2012) 412–427.

[27] S.M. de la Monte, S.A. Lahousse, J. Carter, J.R. Wands, ATP luminescence-based motility-invasion assay, Biotechniques 33 (2002) 98–100 102, 104 passim.

[28] E.T. Roussos, Z. Keckesova, J.D. Haley, D.M. Epstein, R.A. Weinberg, J.S. Condeelis, AACR special conference on epithelial-mesenchymal transition and cancer progression and treatment, Cancer Res. 70 (2010) 7360–7364.

[29] X. Wang, Z. Xin, Y. Xu, J. Ma, Upregulated miRNA-622 inhibited cell proliferation, motility, and invasion via repressing Kirsten rat sarcoma in glioblastoma, Tumour Biol. 37 (2016) 5963–5970.

[30] D.D. Bigner, S.H. Bigner, J. Ponten, B. Westermark, M.S. Mahaley, E. Ruoslahti, H. Herschman, L.F. Eng, C.J. Wikstrand, Heterogeneity of Genotypic and phenotypic characteristics of fifteen permanent cell lines derived from human gliomas, J. Neuropathol. Exp. Neurol. 40 (1981) 201–229.

[31] S. Thomson, F. Petti, I. Sujka-Kwok, P. Mercado, J. Bean, M. Monaghan, S. L. Seymour, G.M. Argast, D.M. Epstein, J.D. Haley, A systems view of epithelial-mesenchymal transition signaling states, Clin. Exp. Metastasis 28 (2011) 137–155.

[32] E.E. Bar, Glioblastoma, cancer stem cells and hypoxia, Brain Pathol. 21 (2011) 119–129.

[33] D.L. Borgas, J.S. Gao, M. Tong, S.M. de la Monte, Potential role of phosphorylation as a regulator of aspartyl-(asparaginyl)-beta-hydroxylase: relevance to infiltrative spread of human hepatocellular carcinoma, Liver Cancer 4 (2015) 139–153.

[34] F. Gundogan, A. Bedoya, J. Gilligan, E. Lau, P. Mark, M.E. De Paepe, S.M. de la Monte, siRNA inhibition of aspartyl-asparaginyl beta-hydroxylase expression impairs cell motility, Notch signaling, and fetal growth, Pathol. Res. Pract. 207 (2011) 545–553.

[35] T. Maeda, P. Sepe, S. Lahousse, S. Tamaki, M. Enjoji, J.R. Wands, S.M. de la Monte, Antisense oligodeoxynucleotides directed against aspartyl (asparaginyl) beta-hydroxylase suppress migration of cholangiocarcinoma cells, J. Hepatol. 38 (2003) 615–622.

 http://dx.doi.org/10.1016/j.heliyon.2016.e00203

[36] H. Yang, K. Song, T. Xue, X.P. Xue, T. Huyan, W. Wang, H. Wang, The distribution and expression profiles of human Aspartyl/Asparaginyl beta-hydroxylase in tumor cell lines and human tissues, Oncol. Rep. 24 (2010) 1257–1264.

[37] Y. Iwagami, C.K. Huang, M.J. Olsen, J.M. Thomas, G. Jang, M. Kim, Q. Lin, R.I. Carlson, C.E. Wagner, X. Dong, J.R. Wands, Aspartate beta-hydroxylase modulates cellular senescence through glycogen synthase kinase 3beta in hepatocellular carcinoma, Hepatology 63 (2016) 1213–1226.

 http://dx.doi.org/10.1016/j.heliyon.2016.e00203